

STRUCTURAL HEALTH MONITORING AND COLD-WORKING VALIDATION USING DMI SR-2 TECHNOLOGY

W.F. Ranson, R.I. Vachon and G.H. Hovis
Direct Measurements, Inc. (DMI)

Results are presented for two separate studies:

The first related to structural health monitoring and CBM and the second life extension/enhancement

The first study conducted by DMI in house and at Northrop Grumman used the DMI SR-2 technology to detect crack initiation and crack growth in 7075-T6 and 2024-T3 and aluminum coupons with holes, both with and without fasteners, subjected to cyclic loading. Hirox images of crack initiation and growth are correlated with the DMI data for the open holes. The results for the cyclic loading studies clearly show the DMI technology detects anomalies, crack initiation and crack growth in fastener holes with and without fasteners. The implication is the DMI SR-2 technology can be used for scheduled and periodic in-the-field inspections of aircraft to evaluate accumulated damage and provide input for CBM. Another implication is the data gathered can be used for design of new aircraft and modifications to existing aircraft.

The second study conducted at the request of NAVAIR involved Fatigue Technology Inc. (FTI) and DMI. The DMI technology was used to evaluate and validate an FTI cold working of a 7075-T6 aluminum coupon. The results clearly show that the measurements of residual strains induced in cold-worked holes indicate the degree of cold working and the absence of residual strains indicates no cold working. The implication of the results is using the DMI SR-2 technology could be used to ensure cold working to a specified degree and permitting a credit for the cold-working process. A most important implication is cold working to a specification can extend the life of critical structural aircraft components.

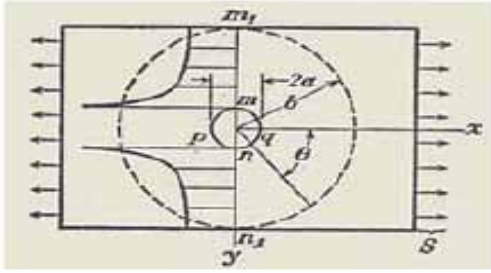
INTRODUCTION:

Residual or plastic strains resulting in critical parts in aircraft from flight environments reflect accumulated damage leading to failure while residual strains induced in fastener holes, cold working, can extend the life of a part. The quantification of residual strain is required in both situations. Measurement of residual strain in critical aircraft parts resulting from flight environments is a prognosis of remaining useful life of the part. Measurement of residual strains resulting from cold working indicates the uniformity of cold working and degree of cold working. Measurements of residual strain using the DMI SR-2 technology are presented for holes in coupons subjected to cyclic loading and cold-worked holes

BACKGROUND TECHNOLOGY

A review of the literature on crack phenomena is helpful to provide background for a discussion of the DMI technology and the results presented.

Timoshenko & Goodier [1] present in the 1951 edition of "Theory of Elasticity" a discussion on the classical solution of the effect of circular holes on stress distribution in plates and cite ten articles on the topic. The figure below presented in [1] illustrates that "the effect of a hole is of a very *localized character*". They show from Saint-Venant's principle that the change in stress distribution "is negligible at distances which are large compared with a , the radius of the hole". Thus, one can conclude that the strain near the



edge of the hole drops quickly as the distance transverse to the applied load increases. This is an important point that dictates that strain measurement relative to the effect of the hole be made as close to the edge of the hole as possible. This is the predicate for the DMI technology to measure elastic and plastic strain on opposing sides at the edge of a hole, determine the differential in the measurements of strain (if any) on each side of the hole and use the differentials to detect crack initiation and monitor crack

growth on the interior lateral surface of the hole. This predicate applies to the validation of cold working.

The literature contains numerous studies on crack growth, crack closure and the role of plastic strain. Elber [2,3,4], Newman and others [5, 6,7,8] have examined various aspects of these topics. Dawicke et. al. [9] looked at three-dimensional crack closure behavior in 2024-T35 aluminum and Newman et. al. [10] studied crack growth in 7075-T7351 aluminum. Schwalbe, Newman and Shannon [11] have studied fracture mechanics testing with inherently low constraint to plastic deformation. In all these studies a crack initiator must be used to seed the crack and plastic strain is the precursor to crack growth. As Elber [3] concluded in a 1970 paper, "At the present stage, it appears that theoretical calculation of the crack closure phenomenon presents great difficulties. Hence, the data required would have to be obtained by experimental means." Further studies on residual stress include those of Ball and Doerfler [12] and Armen et al [13] on fatigue crack growth at cold expanded holes. The Ball and Doerfler study showed photon induced positron annihilation and meandering winding magnetometer arrays were able to detect the presence and degree of cold expansion. The authors state that it "was not clear how the data could be related to stress or strain profiles". The Ball and Doerfler paper has an extensive list of references. The Armen paper concludes that remote compression loads on the residual are significant and omitting the effect of remote compression loads around cold worked holes results in a non conservative crack-growth life prediction. Additionally, the Armen paper concludes that neat-and interference-fit can mitigate "the detrimental effects of remote compression loads on the beneficial residual stresses resulting from coldworking". Recently ASTM International Committee E08 on Fatigue and Fracture has published [14] *Residual Stress Effects on Fatigue and Fracture Testing and Incorporation of Results into Design* which is a collection of papers which include studies of cold-worked holes. The lead-off article in [14] is a FEA of cold-worked holes and discusses that under-prediction of crack growth may lead to premature replacement of a part. The studies on cold-worked holes emphasize the fact that modifying and extending the stress intensity factor, K, to fit cold-worked holes has met with varying degrees of success. It appears that the inability heretofore to measure the residual strain around cold-worked holes and correlate these data with FEA and other analysis techniques hinders predictive models for fatigue life of holes..

The studies to date on crack phenomena and cold working have contributed to the understanding of the phenomena associated with cracks in structures under cyclic loading. However, it appears that despite these many advances there is an un-met role for the measurement of strain as near to the edge of a hole as possible. The promise of the ability to measure plastic strain close to the edge of a hole is to bridge damage mechanics [15] with fracture mechanics. This should give a more complete understanding of crack initiation, crack growth and ultimate total separation of the body containing the hole.

DMI TECHNOLOGY

The Direct Measurements, Inc. (DMI) technology measures plastic (residual) strain and can be used to measure residual strain around holes. The plastic strain is an indication, as a metric pre-cursor to crack initiation in critical parts/components, and the metric to determine accumulated damage and remaining

fatigue life of a part/component. The theoretical developments in Continuum Damage Mechanics [15] since the 1980's have resulted in a unified theory of engineering applications. This theory predicts that damage is governed by accumulated plastic strain beyond a threshold and up to a critical value of the damage variable. The DMI gage technology permits correlation of experimental data with analysis techniques.

Theoretical Basis for DMI Technology

This section discusses the basics of damage mechanics relative to fatigue, the fundamental relation of mechanical deformation related to crack detection and how the DMI technology translates theory into a field ready measurement technique.

A. Total Strain Theory-The total strain of the DMI strain gage as the object undergoes cyclic deformation is fatigue and is mathematically described for total cyclic strain amplitude as

$$\varepsilon_a = \frac{\Delta\varepsilon_e}{2} + \frac{\Delta\varepsilon_p}{2}$$

The total strain life equation in turn is written as

$$\varepsilon_a = \frac{\sigma'_f}{E} (2N_f)^b + \varepsilon'_f (2N_f)^c$$

and total strain in terms of plastic strain

$$\frac{\Delta\varepsilon_p}{2} + \varepsilon_0 \left(\frac{\Delta\varepsilon_p}{2} \right)^{\frac{b}{c}} = \frac{\sigma'_f}{E} (2N_f)^b + \varepsilon'_f (2N_f)^c$$

and strain life in terms of plastic strain can be expressed by

$$\varepsilon_a = \frac{\Delta\varepsilon_p}{2} + \varepsilon_0 \left(\frac{\Delta\varepsilon_p}{2} \right)^{\frac{b}{c}}$$

These equations represent the physical model associated with the deformation of the target. Graphically these equations for strain are shown in FIGURE 1. for 2024-T3 Aluminum below and illustrate that plastic strain is the damage metric. The result shows total cyclic strain is expressed in terms of cyclic lastic strain from strain-controlled fatigue data.

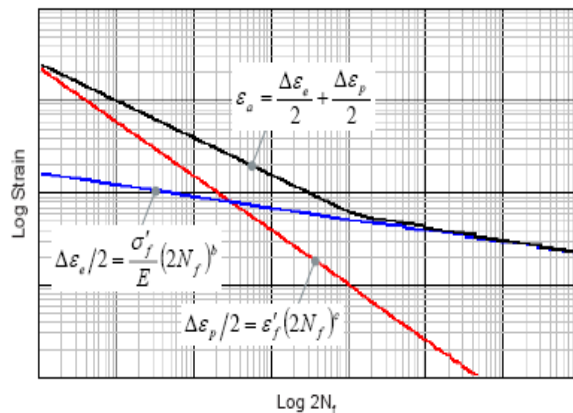


FIGURE 1. Total Strain and Elastic and Plastic Strain

The DMI technology uses strain-controlled data to calculate total strain from measured plastic strains. However, it is the plastic strains that are correlated with the accumulated damage. The utilization of the theory to develop the DMI technology is explained as follows using the fundamentals of the mechanics to achieve the software and hardware to directly measure uniform and non uniform plastic strain. The non-uniform or differential strain is an indicator of an anomaly and crack initiation and growth.

B. Basics of Directly Measuring Uniform and Non-uniform or Differential Strain- The character of deformation in a local region describes parallel lines deform into parallel lines as shown in the Figure 2a below [17] and this restricts the strains to be uniform within in the region. In turn one can illustrate deformation in an area containing an anomaly (Figure 2b).

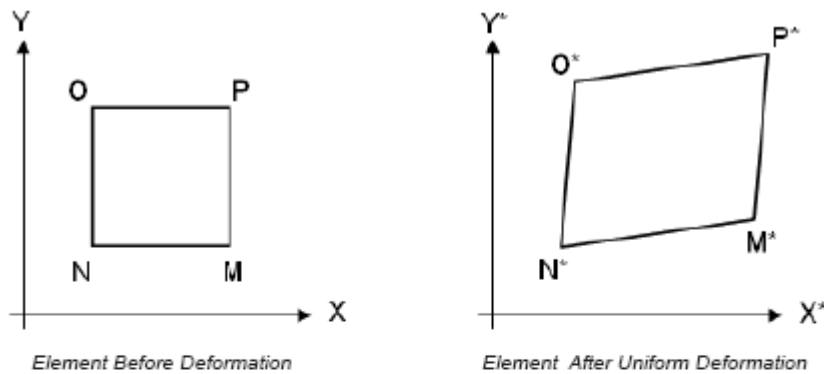


FIGURE 2a. Uniform Element Deformation

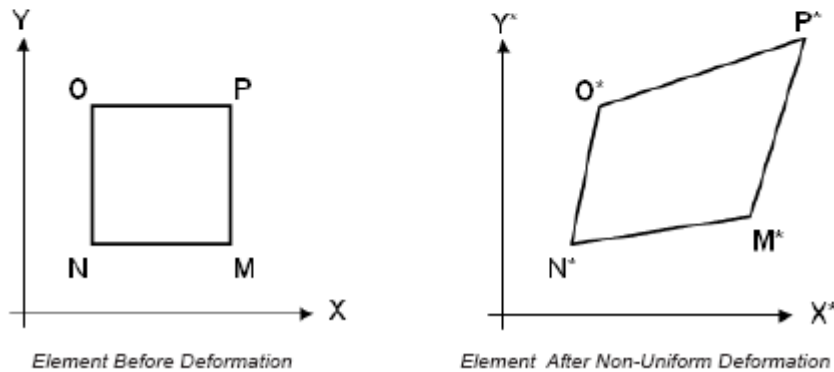
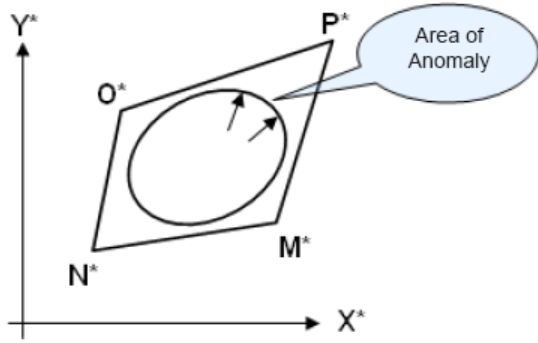


FIGURE 2b. Non-Uniform Element Deformation



DMI Proprietary Gage Centered On Open Hole

As shown in Figure 2b an anomaly leads to non-uniform or differential deformation i.e. the change in O^* to P^* is different than the change in N^* to M^* and the change in N^* to O^* is different from that from M^* to P^*). This fact is a basis for the DMI proprietary gage. The gage measures directly a uniform or non-uniform deformation. A non-uniform or differential deformation of the opposing sides of the gage indicates non-uniform plastic strain (fatigue) or a crack. DMI has demonstrated this experimentally.



Sides of Gage Deformed Non-uniformly and DMI Technology Detects The Difference in Strain in Opposing Sides

Placement of the DMI gage over the center of an open hole permits detection of an anomaly (asymmetric residual strain) or crack based on the non-uniform deformation of the sides. This is illustrated for a test specimen with a DMI gage centered over the open hole as seen on the previous page..

The difference in the strain measured on the opposing sides of the gage as stated indicates the presence of an anomaly. The onset of the difference in the strain on opposing sides of the DMI gage is indicative of the initiation of a crack in a homogeneous material. The arrows point to crack areas. It should be noted that the detection of the location of an anomaly or crack/s is

independent of the orientation of the DMI gage with respect to the direction of the load.

DMI TECHNOLOGY ILLUSTRATED

The DMI technologies (Gage, Software and Hardware) based on engineering mechanics and function are shown schematically and amplified with the inclusion of hardware below

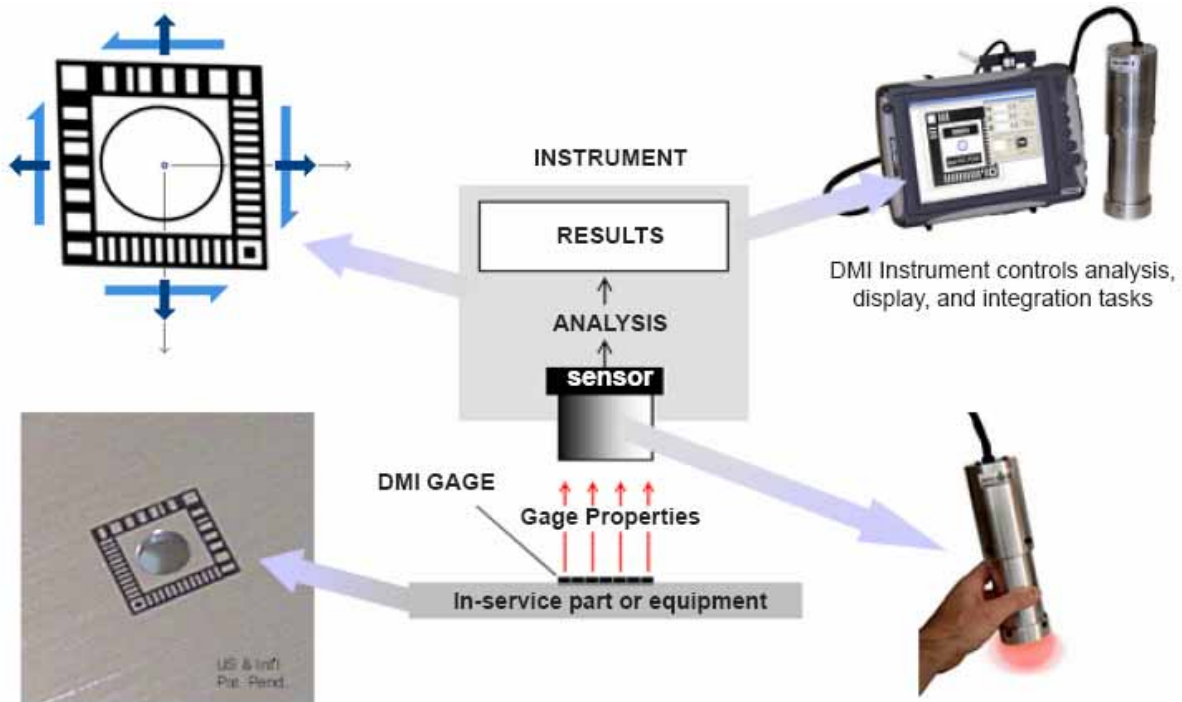


FIGURE 3. Overview of DMI Technologies -How They Work

RESULTS OF EXPERIMENTS TO DETECT CRACK INITIATION & CRACK GROWTH

Tests on Doubler Subjected to Cyclic Loading

DMI has conducted fatigue tests on a doubler test specimen and coupons as seen in FIGURE 4. and has shown that the theory and the DMI technology do indeed indicate the initiation of a crack in a hole

containing a fastener associated with an aircraft structure.

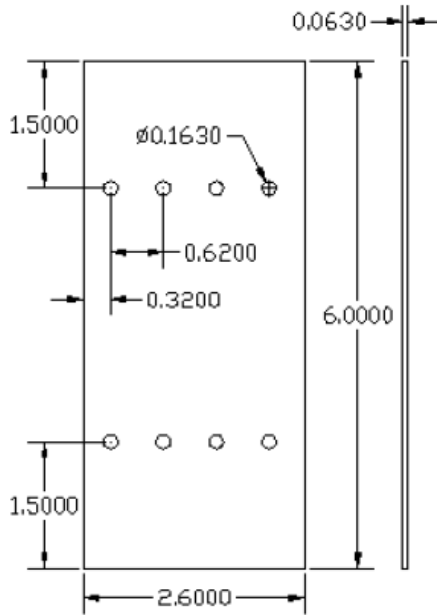


FIGURE 4. Test Specimen Details

The presence of a crack is based on the measurement of the sides of the DMI gage to detect and measure non-uniform deformation of the DMI gage. These results also support the ability to periodically inspect a critical area of an operating aircraft during scheduled or scheduled maintenance. The DMI technology, unlike a wired strain measuring system based on an analog indication of strain, is a direct optical measurement. Thus, the optical reader can be removed and replaced over the DMI gage without the necessity of a recalibration. These tests are described in the following sections.

The significance of the ability to measure non-uniform or differential strains directly and detect anomalies and cracks in open holes using the technology is self evident. The DMI SR technology measures these non-uniform strains directly because of the gage geometry and because the gage can be positioned in the immediate area of the deformation where cracking is anticipated or centered over a hole. The results of the experiments support the use of the DMI technology to detect cracks.

DMI Strain Gages were applied to a fatigue test specimen which were subjected to cyclic loading. The test specimen configuration for the AL7075 T6 doubler is shown FIGURE 4. A doubler was secured with fasteners to each side of two plates (a top plate and bottom plate) separated about 0.5-inch at the center and the jaws of the fatigue machine were clamped to the free end of each plate. Gages 68 and 67 were placed around the top center holes as shown in FIGURE 5.

The SR-1 gages were applied as shown in FIGURE 5. Note that the hole with gage 67 had had a small 0.030-inch starter notch on the left side of the gage prior to testing. The hole with gage 68 did not have a starter notch. The color code around the gage (red vertical right-hand side, blue vertical left-hand side, green horizontal bottom side and brown top side of the gage) is used to correspond with graph colors in Figures 6-11.

The data displayed in Figures 6-11. Initial static data were taken for each gage and Figures 6 and 7 show an almost linear relation for gage 68 and piecewise linear for gage 67 for a load range up to a maximum. Fatigue data were taken at 500 cycle intervals until failure. The test was stopped at each 500 cycle intervals and data recorded at 300 lbs. and 11091 lbs. The data shown in Figures 9 and 11 indicate that gage 67 began to show a difference in strains very easily in the fatigue cycle.

Test Coupon With Fasteners in Holes at Top Center Holes

Typical DMI Gage With Fastener Through Center of Gages 68 & 67

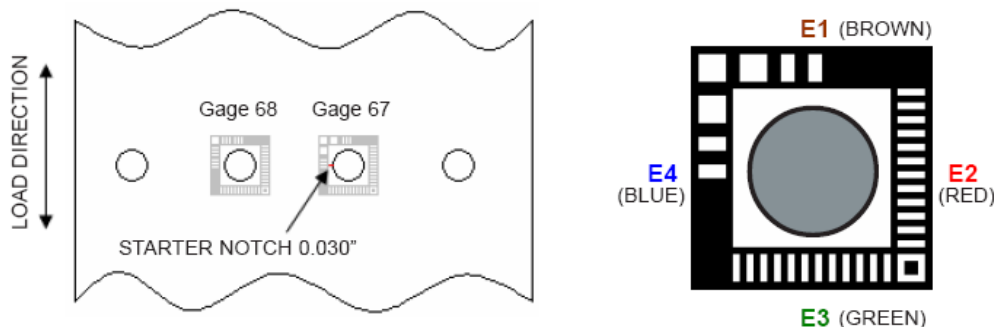


FIGURE 5. Gage Placement on Specimen with Fasteners

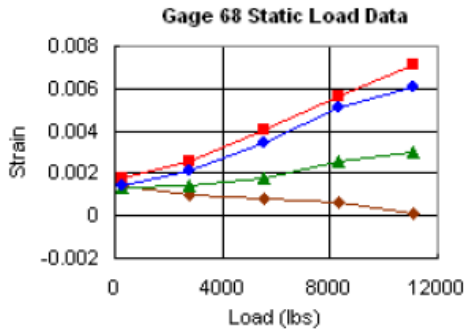


FIGURE 6. Static Load, Gage 68

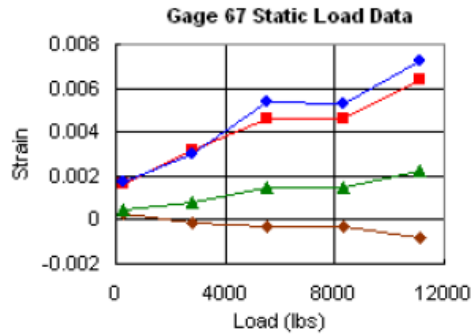


FIGURE 7. Static Load, Gage 67

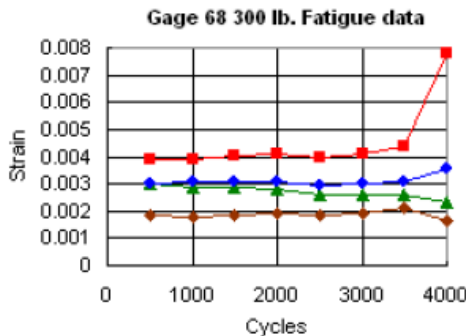


FIGURE 8. Fatigue Data, Gage 68, 300 lbs

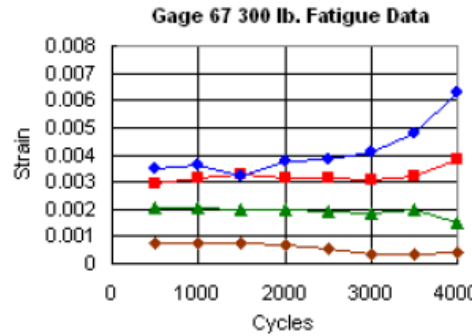


FIGURE 9. Fatigue Data, Gage 67, 300 lbs

As the crack propagated toward gage 68 this gage began to experience the effect of the crack growth toward the outer boundary of the gage. This can be seen in Figure 8 and 10; as the crack began to grow the top blue (E4) and red (E2) curves began to separate. However during this test crack growth was not measured and only general observations can be made at this time.

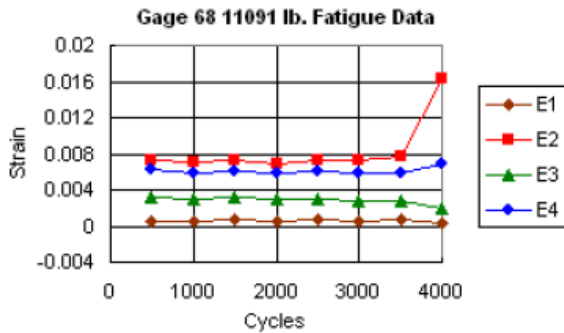


FIGURE 10. Fatigue Data, Gage 68, 11091 lbs

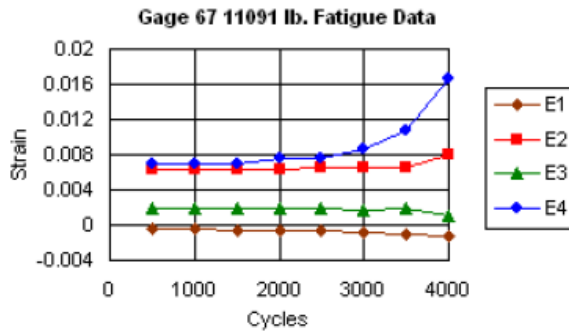


FIGURE 11. Fatigue Data, Gage 67, 11091 lbs

In these tests the fastener heads overlapped inner boundaries of the gages. This prevented determining strain on these inner boundaries. The gage can be made so that the inner boundaries of the gage are tangent to the fastener head as the gage is scalable. This would permit determining the strain on the inner boundary closer to the edge of a hole as discussed in [1] and illustrated by Frocht [36].

Figure 12 is a photoelastic pattern of the stress distribution around a plate loaded through a rivet which closely matched the loading in these tests. As can be observed the gage needs to be located as near the rivet head as possible.



FIGURE 12. Pin in the Hole of Plate Loaded by a Force on the Pin

Furthermore the stresses are nearly uniform in this outer region. The fastener heads prevented a gage measurement at the critical point at the inner boundary of the hole. However , a gage measurement relatively close to the critical point can be made ,if an inner boundary of the gage is used. Figure 12 is used to illustrate the stress distribution in a qualitative manner and is not to be used as a direct comparison.

Tests on Fatigue Coupons Subjected To Cyclic Loading

DMI Strain Gages were applied to two Northrop Grumman fatigue coupons which were subjected to cyclic loading in the Northrop Grumman Bethpage testing facilities. The gages were monitored after successive cyclic loading of the 13DMI389 and 13DMI397 coupons. Results were obtained for strain and corresponding Hirox images. This work approved for public Release, Distribution Unlimited-DISTAR 7995. The results are presented as follows:

A. Preliminary Data Analysis for 13DMI389/SIPS S13-0389 (DMI Encoded Gage 24)

Fatigue testing was performed on Northrop Grumman Coupon SIPS S13-0389 with two holes near the coupon's center. DMI gages were affixed over both hole locations (locations "1" and "2" in Figure 13) and drilled through so holes in coupon and the holes in the gage were concentric with the same diameter-0.190-inch. This analysis deals with the DMI gage on the left-hand side of the fatigue coupon, which is labeled "1". This particular DMI gage has an encoded serial number of 24, and is referred to herein as "gage 24."The early fatigue crack initiated on the is encoded as Gage 25 and was not monitored during this outboard left side of this gage location. The right hand side gage test.



FIGURE 13. Fatigue test coupon with DMI

In these tests, the random fatigue loading spectrum was specified by Northrop Grumman. At specified intervals load cycling was stopped, a preload was applied, and cracks were measured using the Hirox microscope. At each hold point, strains were recorded at gage 24 using DMI's handheld strain reading instrument. The first gage reading was recorded at 6500 cycles which corresponded to a minimum crack size as determined by an independent measurement with a JENTEK device. Count 6 was recorded at 7000 cycles and strains compared to the base reading at 6500 cycles. All subsequent count readings were recorded at 500 cycle intervals up to 9500 cycles.

The strain readings at the first point (count 6 or 6500 cycles) indicate parallel sides are experiencing approximate equal and uniform conditions relative to the base reading. At count 6 the DMI instrument reported axial and transverse strains consistent with a pre-crack material response to the applied loads. The DMI instrument also reported a small shear strain at count 6, which is further evidence that principal directions are in the load and transverse directions and that there is no indication of a crack.

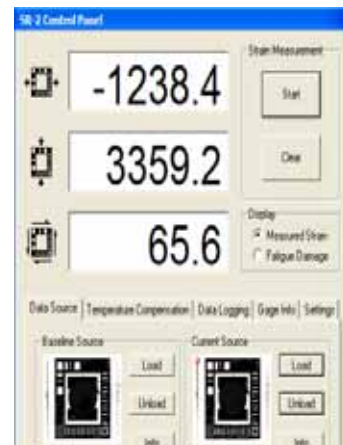


Figure 14 is an instrument display of the strain data. The strains in the direction of load and the transverse direction are consistent with the measure of plastic strain components. However, since the base image was recorded with a small crack and not an un-deformed configuration this early measurement is expected. An un-deformed baseline image should reveal the early plastic strains prior to the crack growth

Figure 15 shows the gage 24 data recorded at the specified hold points. DMI's instrument records the strain along all four side of the gage. These four simultaneous readings are plotted on individual lines in Figure 15. As expected, the left and right extensional strains (blue and red lines) are large, positive values, as these sides are parallel to the direction of loading. FIGURE14. Instrument Display

The readings along the gage top and bottom (green and brown lines) show the expected compressive strains, as they are measured in a direction transverse to the applied loads. Initial crack formed on the outboard side of gage 24 which corresponds to the blue line. Strain difference between the blue and red lines is an indication of crack opening displacements between a cracked line (blue) and a non-cracked line (red). As fatigue cycles increase, the DMI readings indicate that strains are no longer uniform and equal on parallel sides. Beginning with count 7 and continuing to count 11, strains on the left and right sides continue to separate with increasing cycles until the test was terminated. These preliminary data suggest that when a crack begins to form the parallel lines of strains will begin to bifurcate; a trend that continues until failure. The transverse curves also reveal the same type of behavior although not as pronounced. The transverse curves also suggest that the crack did not form along a line of symmetry.

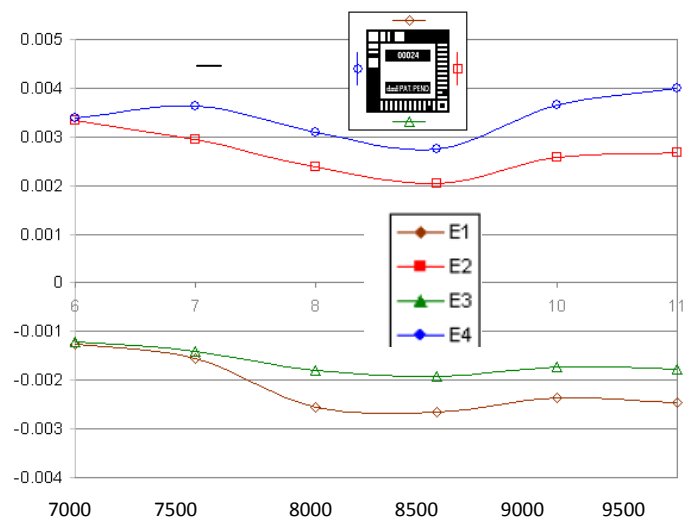


FIGURE15. DMI strain readings vs cyclic count

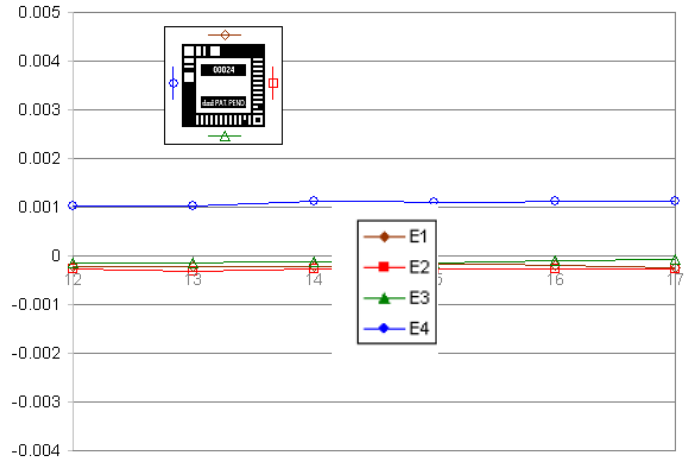
Photographs taken after the test (i.e. after count 11) show a crack on the back side of the fatigue coupon in the location indicated by the left-side strain data from the DMI gage. This image is shown in Figure 16. This visible crack formed just below the centerline of the hole, which is consistent with a larger transverse strain magnitude along the gage top (brown line in Figure 15).



The test was terminated before fracture, and the coupon was removed from the load frame. After the test was terminated at 9500 cycles the coupon was removed from the fatigue machine and multiple readings were made at zero load. Strains were again recorded with the DMI instrument at gage 24, now at a zero load state corresponding to 9500 cycles.

FIGURE 16. Crack location on back side of gage 24.

This test was performed in order to determine if the fatigue damage could be detected by the DMI instrument and gage at zero load. This series of readings was made to determine measurement repeatability and strains at zero loads. Figure 17 shows that at zero load, the strains along the top, right, and bottom sides of gage 24 returned to near a zero reading. The left-side strain reading reports a large magnitude fixed strain on the edge with the crack. A comparison of the non-uniform strains at 9500 cycles in Figure 15 to the non-uniform strain values in Figure 17 yields essentially the same results. This information suggests the possibility that gage readings of this type could be developed into an inspection procedure where measurements are made at zero load.



B.. Preliminary Data Analysis for 13DMI397/SIPS S13-0397 (DMI Encoded Gage 28)

A fatigue test was performed on Northrop Grumman Coupon SIPS S13-0397 with a single hole in the center of the plate. DMI Gage 28 was affixed over the hole location and drilled through so the hole in coupon and the hole in the gage were concentric with the same diameter, 0.190-inch. The fatigue loading was constant amplitude (zero to tension) and the amplitude was specified by NG personnel. The initial phase of the test was to develop a test protocol and test the bondable gage under fatigue loading. A base line recording was made with the coupon at zero load. At specified intervals load cycling was stopped, a preload was applied, and cracks were measured using the Hirox microscope. At each hold point, strains were recorded at gage 28 using DMI's handheld strain reading instrument. The strain readings for this coupon were recorded in the latter stages of the fatigue test and denoted as counts 1-5. Figure 18 shows the strain values plotted in the same manner as gage 24.

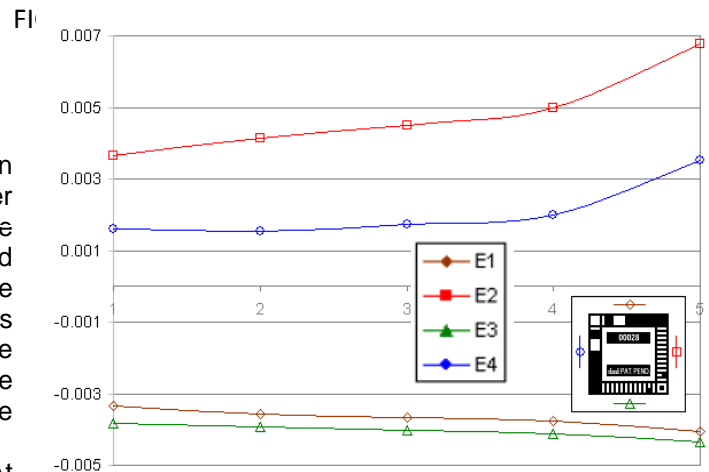


FIGURE 18. Strain readings vs count

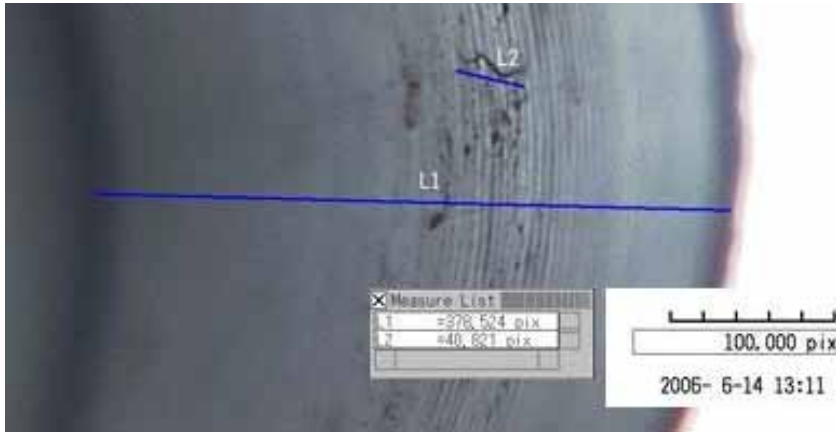
In this test the fatigue crack was initiated on the right side of the hole (red line). After the test was completed the coupon was cycled until failure to further test the durability of the gage. As can be seen in this photograph (Figure 19) the gage remained bonded after failure; demonstrates the adhesive qualities of the DMI Gage.



FIGURE 19 Fatigue Coupon after failure

B. Comparison of the Strain Data with the Hirox Images for 13DMI389 (DMI Encoded Gage 24)

Figure 20 (a-b) shows the crack growth on the internal lateral surface (bore) of the outboard side of the 13DMI 389 coupon from images captured with a Hirox microscope. An initial image, based on the JENTEK sensor indication of crack, was taken at 6500 cycles and subsequent images were recorded at 500cycle intervals.



The test was terminated at 9500 cycles. Gage 24 strain readings shown in Figure 15 correlate with the Hirox images at these cycle intervals. Hirox image, Figure 20 a. , is shown at 6500 cycles and the last HIROX image is Figure 20 b. The complete set of HIROX images show the crack starts near the center and grows toward the opposite side of the DMI gage.

FIGURE 20 a. Hirox images of the crack in coupon S13-0389 location1 (gage 24) vs. number of cycles (S13-0389 H1 OB 6500cycles 10K load)

FIGURE 20 b. Shows the crack has progressed from the interior lateral surface to the exterior surface of the coupon

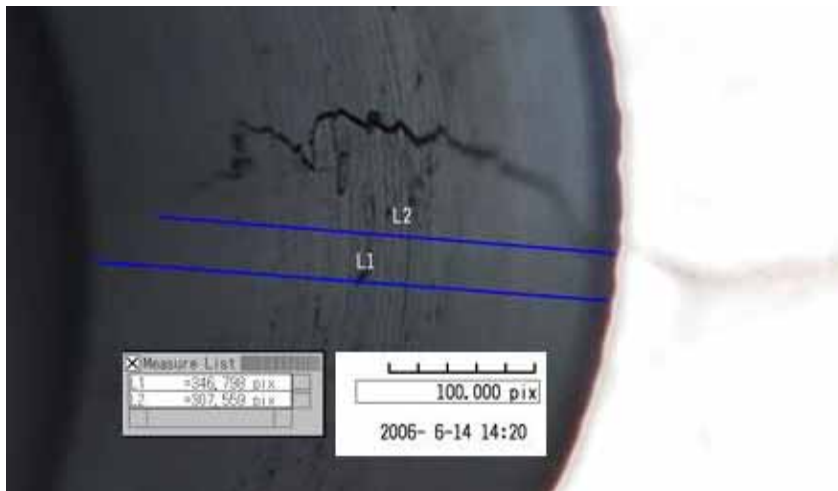


FIGURE 20 b. Hirox images of the crack in coupon S13-0389 location (gage 24) vs. number of cycles (S13-0389 H1 OB 9500cycles 10K load)

C. Comparison of Hirox Data with Crack Length and Strain Data

Figure 21. shows the crack length in inch vs number of cycles. Although the data is limited, the plot clearly displays the trend of increasing crack length with the increasing number of cycles.

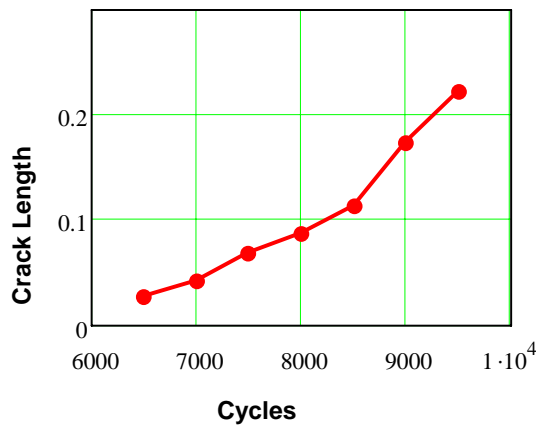


FIGURE 21. CRACK LENGTH (INCH) VS. CYCLES

Strains were recorded along each line of the gage surrounding the open hole as shown in Figure 22. The crack formed along the left side of the gage which is shown in the lower left vertical leg of the gage. These readings were then compared with the vertical readings on the right leg of the gage (second from the top). These two readings are shown as the red and blue lines in Figure 15.

Figure 23 is a plot of the measured strain difference readings in microstrain between the left (crack side) and right side elements vs. measured crack length in inch corresponding to each independent measurement from 6500 – 9500 cycles at 500 cycle intervals. Strain differences were calculated from the data shown in Figure 15 and the crack length measurements were calculated from the HIROX data.

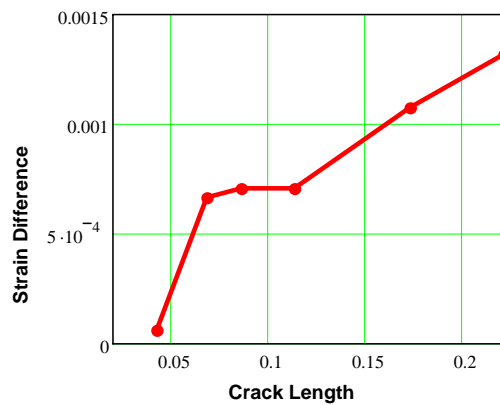


FIGURE 23 STRAIN DIFFERENCE (MICROSTRAIN) VS. CRACK LENGTH (INCH)

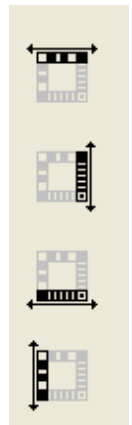


FIGURE 22 Strain Read On each side of gage

Findings and Conclusions

Based on the technical methodology the emphasis was on basic experiments. These experiments were to demonstrate the utility of the DMI technology to measure strain around a hole with a fastener in a plate subjected to cyclic loading and crack growth in the hole and ultimately to the surface of the plate. A number of studies were used [14 to 25] to form a background for the study in addition to those cited earlier. Specific findings and conclusions include:

1. The tests demonstrated the utility of the DMI technology to monitor crack growth and measure differential strain around the hole in a plate with and without a fastener subjected to cyclic loading

2. In the experiments two edges of the gage were parallel to the direction of cyclic loading. It is important to note that the orientation of the gage and its ability to detect crack initiation and crack growth is independent of orientation of the gage, because the gage measures orthogonal extensional strains and associated shear strains. This is important in that other crack detection technologies must have a specific orientation of the sensor with respect to the direction of the load to detect a crack in a hole.

3. The tests suggest that holes containing fasteners can be tested and crack growth can be monitored when the DMI gage is centered on the hole containing the fastener with the interior edges tangent to the hole containing the fastener. This suggestion is based on fundamental work conducted in the 1930s and 40s [26,27,28, 29,30,31].

4. The DMI technology permits periodic inspection of a DMI gage centered on a hole containing a fastener on in-service equipment to determine the presence of cracks at scheduled inspection intervals or after an unusual loading. This would be useful for aircraft inspection subsequent to a "hard" landing or "extreme" flight conditions. Periodic inspection is based on the fact that the DMI reader can be removed and placed on the DMI gage at any subsequent time as the plastic strain event is "recorded" in the gage.

5. A pattern of DMI gages can be used to measure a strain field.

6. Measurement of surface strain in a surface with fastener holes containing fasteners is more informative with DMI gages centered on the fastener holes than using electrical resistance gages since the DMI gages can detect strain close to the hole where strain is high. This comment is based on the discussion by Timoshenko and Goodier cited above. This does not mean that electrical resistance gages do not have a role. It suggests that electrical resistance gages may be more economically and technologically informative, if deployed differently than currently deployed on surfaces with fastener holes.

RESULTS OF EXPERIMENTS TO MEASURE THE DEGREE OF COLD WORKING

Fatigue Technology ,Inc. (FTI) provided Direct Measurements, (DMI) a 7075-T6 specimen with five fastener holes. DMI applied the DMI wire-free strain gage around each hole as shown in Figure 24 (front). The specimen was returned to FTI for cold work Prescribed expansion according to Table 1. After FTI Completed cold work expansion, the specimen was returned to DMI for residual strain measurements. This summary presents the results of the residual strain measurements and shows the applicability of the DMI strain measurements to quantify the FTI cold expansion technology.

Hole #	Cx Type	DMI Gage #
1	None	95
2	2% Cx(Under Expanded)	96
3	CB Min.(Min. Standard)	97
4	CB Max. (Max. Standard)	98
5	CA Nom. (Over Expanded)	99

Table 1 Cold Work by Hole and Gage Number

Residual strain measurements were made on both the inner and outer boundary of each gage and measured strain components E1 (brown),E2 (red), E3 (green), E4 (blue) were recorded according to the Figure 25. The holes and corresponding gage codes are shown in Table 1 and Figure 24.

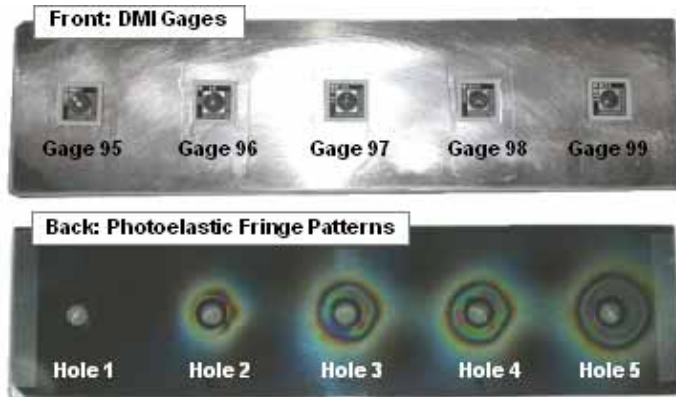


Figure 24. 7075-T6 Test specimen Front and Back



Figure 25. Gage 96 Surrounding Hole 2

The DMI gage outer boundary measurements are shown in Figure 26. Which demonstrates that the residual strain magnitudes follow the trend in photoelastic patterns in Figure1 (back). Note that the right-hand side fringe order is slightly higher in holes 3,4 and 5. Accordingly, the strain component E2 (red) measured on the right-hand side of gages 97, 98 and 99 is also slightly higher. In this figure, gage 98 fails to indicate a higher E2 components due to inner-boundary gage damage during cold- work expansion. Nonetheless, the remaining components give sufficient indication of the degree of cold working. In addition , DMI gages can be produced with dimensions that better match holes sizes, thereby avoiding damage.

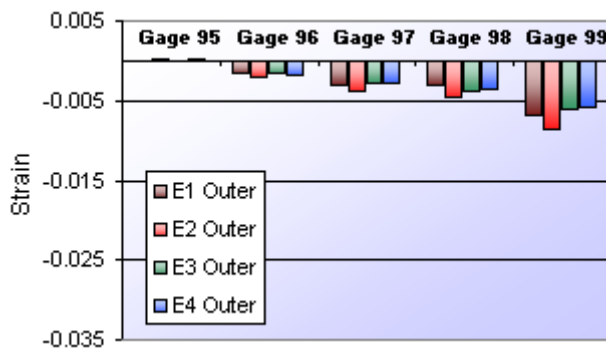


Figure 26. DMI gage Readings on Outer Boundary

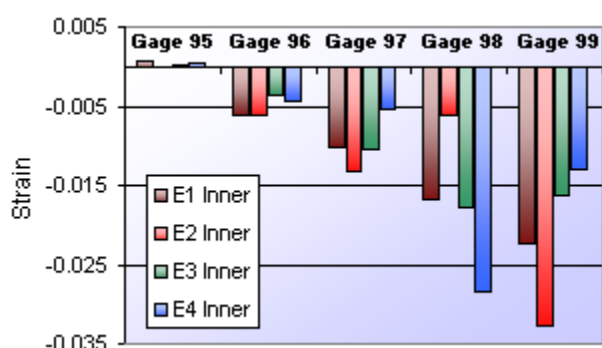


Figure 27. DMI Gage Readings on Inner Boundary

Findings and Conclusions

The results indicate the DMI strain measurement technology provides a viable means of quantifying cold-work expansion. The measurements were qualitative in nature and were not intended as direct comparison of the independent measurements.

REFERENCES

- [1] S. Timoshenko and J.N. Goodier, *Theory of Elasticity* McGraw-Hill Book Company, Inc. New York, 1951
- [2] W. Elber, Fatigue Crack Propagation, Ph.D. Thesis, University of N.S.W., Australia, 1968
- [3] W. Elber, Fatigue Crack under Closure Cyclic Tension, *Eng. Frac. Mech.*, 3,37-34 (1970)
- [4] W. Elber, The Significance of fatigue crack Closure, *Damage Tolerance in Aircraft Structures*, ASTM STP 748, 53-84(1981)
- [5] J.C. Newman Jr., M. Jordan Haines, Verification of stress-intensity factors for various middle-crack tension test specimens, *Eng. Frac. Mech.*, 72, 1113-11,(2005)
- [6] Kiran Solanki, S.R. Daniewicz, Jc. Newman Jr., Finite element analysis of plasticity-induced fatigue crack closure: an overview, *Eng. Frac. Mech.*, 71,149-171 (2004)
- [7] S.K. Ray, R Perez , A.F. Grandt Jr., *Fatigue and Fracture of Engineering Materials and Structures*, 10 (3),239-250,(1987)
- [8] A.I. Rifani, A.F. Grandt, Jr., A FRACTURE MECHANICS ANALYSIS OF FATIGUE CRACK GROWTH IN A COMPLEX CROSS SECTION, *Engineering Failure Analysis*, Vol 3., No. 4 249-265 (1996)
- [9] D. S. Dawicke, A. F. Grandt Jr., and J.C. Newman Jr. THREE-DIMENSIONAL CRACK CLOSURE BEHAVIOR, *Eng. Frac. Mech.*, Vol. 36, No. 1, 11-121 (1990)
- [10] J.C. Newman Jr., A. Brot, C. Matias, Crack-growth Calculations in 7075-T7351 aluminum alloy under various load spectra using an improved crack-closure model, *Eng. Frac. Mech.* , 7, 2347-2363 (2004)
- [11] Karl-Heniz Schwalbe, Jams C. Newman Jr, John L. Shannon Jr. , Fracture mechanics testing on specimen with low constraint-standardisation activities within ISO and ASTM, *Eng. Frac. Mech.* ,72 557-576 (2005)
- [12] Dale L. Ball and Mark T. Doerfler, Experimental and Analytical Studies of Residual Stress Field Evolution and Fatigue Crack Growth at Cold Expanded Holes , 2003 USAF ASIP Conference Savannah, GA Dec 2003
- [13] H. Armen, Alvin Levy, and H.L. Eidinoff, Elastic-Plastic Behavior of Cold worked Holes, Paper 83-0865 AIAA 24th Structures, Structural Dynamics, and Materials Conference, Lake Tahoe, NV, May 2-4 1983
- [14] Jeffrey O. Bunch and M.R. Mitchell, editors, Residual Stress Effects on Fatigue and Fracture Testing and Incorporation into Design, ASTM STP 1497, West Conshohocken, PA 2007
- [15] J. Lemaitre, *A Course on Damage Mechanics*, Second Edition Springer-Verlag, Berlin, 1996
- [16] W.F. Chen, D. J. Han, *Plasticity for Structural Engineers*, Gau Lih Book Co., Ltd., 1995.
- [17]. V. Novozhilov, *Foundations of the Non Linear Theory of Elasticity*, Graylock Press, New York, 1953.
- [18] M. Carboni, Stain-gauge compliance measurements near the crack tip for crack closure evaluation: Applicability and accuracy, *Eng Frac. Mech* , to be published based on being accepted 19 April 2006

- [19]. K.H.Schwalbe, Estimating the load line displacement of cracked laboratory specimen using the engineering treatment, *Eng Fract Mech*, 45 (1993) (6), 751-758.
- [20]. K.H.Schwalbe, B. Hayes, K. Baustain *et al*, Validation of the fracture mechanics test method EGF P1-87d (ESIS P1-92). *Fatigue Fract. Eng Mater Struc*, pp1231-1284, 1993.
- [21]. W. Mekky, P.S. Nicholson, The fracture toughness of Ni/Al₂O₃ laminates by digital image correlation I: experimental crack opening displacement and R-curves, *Eng Fract Mech*, 73, (2006), (5), 571-582.
- [22]. L.J. Fellows, D. Nowell, Measurement of crack closure after the application of an overload cycle, using moiré' interferometry, *Inter J Fatig*, 27, 2005, (10-12), 1453-1462,.
- [23]. P. Hung, A. S. Voloshin, In-plane strain measurements by digital image correlation, *J Braz Soc Mech Sci. Engng*, XXV,(2003), (3), 215-221.
- [24]. D. Amodio, G.B. Broggiato, F. Campana, G. M. Newaz, Digital speckle correlation for strain measurement by image analysis, *Soc Exp Mech*, 43 (2003) (4), 396-402.
- [25]. M.A. Sutton, F. Ma, X. Deng, Development and application of a CTOD based mixed mode fracture criterion, *Int J Solids Struct* 37 (2000), 3591-3618.
- [26]. F. Hild, Measuring stress intensity factors with a camera: integrated digital image correlation (I-DIC), *Comptes Rendus Mécanique*, 334, 2006 (1), 8-12.
- [27]. J.D. Helm, M.A. Sutton, S.R. McNeill, Deformations in wide, center-notched panels, part I: three-dimensional shape and deformation measurements by computer vision, *Optical Engineering*, 42, 2003 (12), 1293-1305.
- [28] J. Lemaitre, *A Course Damage Mechanics*, Springer –Verlag, 2nd Edition, Berlin, (1991)
- [29]. M.A. Sutton, A.P. Reynolds, J. Yan, B. Yang, Microstructure and mixed mode I/II fracture of AA2524-T351 base material and friction stir welds, *Eng Fract Mech*, 73, 2006 (4), 391-407.
- [30] K. Sezawa and G Nishimura, Rept. Aeronaut. Research Inst.. *Toyko Imp. Univ.*, vol. 6. no. 25, (1931)
- [31] J. N. Goodier, *Trans. A.S.M.E.*, vol.55, 39 (1933)
- [32] L. H. Donnell, Theodore von Karman Anniversary Volume, Pasadena, 293, (1941)
- [33] E. Thibodeau, L.A. Wood, *J. Research Natl. Bur. Standards*, vol. 20, 393, (1938)
- [34] A.E. Green, *Trans. Roy Soc(London)*, series A, vol. 103, 229
- [35] E. Sternberg, M. Sadowsky, *J. Applied Mechanics (Tans. A.S.M.E.)*, vol. 16,27, (1949)
- [36] Max Mark Frocht , *Photoelasticity* , John Wiley & Sons Inc. , 8th Printing ,New York, ., 1966